Eur Biophys J (1996) 24: 413–421

ARTICLE

Laurent Girault · Philippe Lemaire · Alain Boudou
Jean-Claude Debouzy · Erick J. Dufourc

Interactions of inorganic mercury with phospholipid micelles and model membranes. A ^{31}P-NMR study

Received: 2 February 1996 / Accepted: 30 April 1996

Abstract The binding of inorganic mercury Hg(II) to phospholipid headgroups has been investigated by phosphorus-31 nuclear magnetic resonance of phosphatidylethanolamine (PE), phosphatidylserine (PS) and phosphatidylcholine (PC) in water micellar and multilamellar phases. $HgCl_2$ triggers the aggregation of phospholipid micelles, leading to a lipid-mercury precipitate that is no longer detectable by high-resolution ^{31}P-NMR. The remaining signal area corresponds to micelles in the soluble fraction and is a non-linear function of the initial mercury-to-lipid molar ratio. Kinetics of micelle aggregation are exponential for the first 15 min and show a plateau tendency after 120 min. Apparent Hg(II) affinities for phospholipid headgroups are in the order: PE > PS > PC. The same binding specificity is observed when $HgCl_2$ is added to (1:1) mixtures of different micelles (PE + PC; PS + PC). However, mercury binding to mixed micelles prepared with two lipids (PE/PC or PS/PC) induces the aggregation of both lipids. Hg(II) also leads to a ^{31}P-NMR chemical shift anisotropy decrease of PC, PS and mixed (1:1) PE/PC multilamellar vesicles and markedly broadens PS spectra. This indicates that $HgCl_2$ binding forces phospholipid headgroups to reorient and that the concomitant network formation leads to a slowing down of PS membrane collective motions. Formation of a gel-like lamellar phase characterized by a broad NMR linewidth is also observed upon $HgCl_2$ binding to PE samples both in fluid (L_α) or hexagonal (H_{II}) phases. The PE hexagonal phase is no longer detected in the presence of $HgCl_2$. Mixed PE/PC dispersions remain in the fluid phase upon mercury addition, indicating that no phase separation occurs. Addition of excess NaCl leads to the appearance of the non-reactive species $HgCl_4^{2-}$ and induces the reversal of all the above effects.

Key words ^{31}P-NMR · Inorganic mercury · Phospholipids · Toxicity · Biomembranes

Abbreviations A(t), time-dependence of peak area: A_{40}, peak area at t = 40 min; $1/\beta$, rate of peak area decrease; δ, isotropic chemical shift; $\Delta\delta$, isotropic chemical shift change; $\Delta\sigma$, chemical shift anisotropy; DPPC, dipalmitoylphosphatidylcholine; Hg(II), inorganic mercury; NMR, nuclear magnetic resonance; pCl, –log [Cl^-]; PC, phosphatidylcholine; PE, phosphatidylethanolamine; PL, phospholipid; PS, phosphatidylserine; R_i, mercury-to-lipid molar ratio; MLV, multilamellar vesicles; SUV, small unilamellar vesicles.

1. Introduction

Epithelial barriers and biological membranes are the initial targets for pollutants from the surrounding environment. Interactions of pollutants with biomembranes also control their uptake processes and subsequent toxicological effects at the cell and organ levels (Boudou et al. 1991; Foulkes and Bergman 1993). Understanding the mechanisms controlling these interactions at the molecular level is therefore of primary importance to interpret the results of bioaccumulation and toxicological studies on various biological models (Rothstein 1976). Both organic and inorganic mercury compounds display strong thioloprive properties, i.e. they bind to membranous and intracellular proteins, inducing severe disturbances of essential membrane properties which may lead to cellular death (Ralston and Crisp 1981; Sharma et al. 1981; Chávez and Holguín 1988). However, proteic thiol ligands cannot account for the total mercury binding to biomembranes, as first discussed by

L. Girault · E. J. Dufourc (✉)
Centre de Recherche Paul Pascal, CNRS, Avenue A. Schweitzer, F-33600 Pessac, France

L. Girault · A. Boudou
Laboratoire d'Ecotoxicologie, Université Bordeux I/CNRS, F-33405 Talence, France

P. Lemaire
Elf Altochem, Service Analyse Environnement, F-92303 Levallois-Perret, France

J.-C. Debouzy
Centre de Recherche du Service de Santé des Armées, F-38702 La Tronche, France

Kinter and Pritchard (1977). It has been suggested that mercury interactions with membrane lipids could be responsible for lipid peroxidation (Ribarov and Benov 1981) and membrane rigidification phenomena (Delnomdedieu et al. 1989; Boadi et al. 1992), but so far little is known about mercury-lipid interactions at the molecular level, except that they depend strongly on the chemical form of the metal (Hg°, Hg(II), $CH_3Hg(II)$,...) and on its reactions in the dissolved phase (Gutknecht 1981; Bevan et al. 1983; Stáry and Kratzer 1989; Farrell et al. 1993). Recently, Shinada et al. (1991) and Delnomdedieu et al. (1992) have shown by ^{1}H- and ^{199}Hg-Nuclear Magnetic Resonance that the electro-neutral $HgCl_2$ species specifically binds to phosphatidylserine and phosphatidylethanolamine multilamellar vesicles through a non-electrostatic interaction, the primary amine groups of PE and PS polar heads being proposed as the mercury binding sites. Quantitative analysis of ^{199}Hg-NMR data allowed calculation of affinity constants and stoichiometrics for the metal/lipid complexes (Delnomdedieu et al. 1992).

To reach a better understanding of inorganic mercury interactions with the headgroups of biomembrane phospholipids, ^{31}P-NMR of phosphatidylethanolamine, phosphatidylserine and phosphatidylcholine in micellar and multilamellar form has been performed under controlled physico-chemical conditions, in the presence and absence of $HgCl_2$. Micelles were chosen because they yield isotropic lines in high-resolution ^{31}P-NMR, allowing one to differentiate between the several phospholipid species (PE, PS, PC), and because it has been proposed that the micellar phase gives binding parameters which are similar to those obtained with multilamellar vesicles (Tacnet et al. 1991). Inorganic mercury effects on micelles prepared with one or two lipids and on mixtures of two homogenous micelle preparations have been compared, in order to study competitive mercury binding to the different phospholipid headgroups. The kinetics and metal-to-lipid molar ratio dependence of these interactions have also been explored. Because multilamellar vesicles are good models of protein- free membranes ^{31}P-NMR of MLV has also been performed to investigate the specific role of the lipid bilayer organization on the interaction and to show the consequences of mercury binding on membrane structure.

2. Materials and methods

Materials

$HgCl_2$, CH_3COONa, CH_3COOH and Triton X-100 were obtained from Prolabo (France), egg yolk PE from Lipid Products (UK) and bovine brain PS from Fluka (Switzerland). Egg yolk PC was prepared according to the method of Singleton et al. (1965) and dipalmitoylphosphatidylcholine (DPPC) was obtained from Sigma (USA). Deionized water with chloride concentration $[Cl^-] < 10^{-5}$ M was used for buffer preparation. Chloride concentration values in the samples were measured using a chloride selective electrode (Orion, Switzerland). All other compounds were high purity reagents from Prolabo (France).

Sample preparation

Phospholipids (PL) were dissolved in $CHCl_3$ and kept at −18 °C. To obtain multilamellar vesicles, the solvent was evaporated under a nitrogen stream and the residue pumped under vacuum to remove traces. Samples were dispersed in acetate buffer (74 mM, pH 5.8) by performing several freeze-thaw cycles and vortex stirring. To form (1:1) PE/PC MLV, aliquots of PE and PC in $CHCl_3$ were first mixed together, then the solvent was evaporated and the phospholipids re-dispersed in buffer as described above. Micellar phases (15 mM) were prepared by Triton X-100 addition (10% weight/volume) to the lipid dispersions and stirring (Tacnet et al. 1991). Two-lipid (1:1) micelle samples were prepared either by mixing micelles made of only one phospholipid species or by forming two-component mixed micelles. To obtain mixtures of two different micellar phospholipids (PL1 + PL2), each lipid aliquot in $CHCl_3$ was separately evaporated, dispersed in acetate buffer and solubilized with Triton X-100. Both micellar preparations were mixed together to obtain 15 mM individual lipid concentration. Mixed micelles composed of two different phospholipids (PL1/PL2, 15 mM each) were prepared by mixing and stirring together both lipid aliquots in $CHCl_3$, followed by evaporation, dispersion, and solubilization by Triton X-100.

$HgCl_2$ was added to phospholipids at defined molar ratios ($R_i = [Hg]/[PL]$) from two stock solutions (50 mM or 200 mM, in acetate buffer). R_i values ranged from 0 to 3.5, with corresponding Hg(II) concentrations from 0 to 52.5 mM. For the two-lipid samples, R_i was calculated with respect to each individual lipid. Assuming that chloride, hydroxide and acetate ions are the only Hg(II) ligands to be considered in solution, chemical models based on available thermodynamic data (Schecher and McAvoy 1991; Delnomdedieu et al. 1992) predict that the soluble $HgCl_2$ species accounts for at least 95% of total Hg(II) under our experimental conditions: pH = 5.8 and pCl = 2.7 to 2.9, depending on total $[HgCl_2]$. The remaining 5% is present as HgClOH and $HgCl_3^-$, the limited $HgCl_2$ dissociation being the main source of free chloride ions. To study the influence of chemical speciation on mercury-lipid binding, the supernatant which appears in the NMR tubes after a few hours was removed and replaced by acetate buffer saturated with NaCl (6.2 M). Under these conditions (pCl = −0.8), 100% of Hg(II) should be present as the negatively charged $HgCl_4^{2-}$ species (Schecher and McAvoy 1991; Delnomdedieu et al. 1992). Non-specific, Na^+-induced micelle aggregation prevented the use of NaCl with micellar samples.

NMR

^{31}P-NMR spectra of phospholipid lamellar phases were recorded at 162 MHz with the Hahn-echo sequence (Rance

and Byrd 1983) under ^1H spin lock decoupling conditions, on a Bruker AM 400 spectrometer operating in unlocked mode, with 5 mm diameter NMR tubes. Signals were acquired using a 50 kHz spectral window, 1600 scans, 10 μs $\pi/2$ pulses, 6 s recycle time and a 30 μs delay between pulses to form the echo. A Lorentzian line broadening of 100 Hz was applied to the FID before Fourier transformation. Temperature was regulated to ±1 °C.

^{31}P-NMR spectra of phospholipids in micelles were recorded at 296 K on a Bruker WH 270 spectrometer, operating at 109.35 MHz in unlocked mode, with the single pulse acquisition sequence. Samples enclosed in 5 mm tubes were spun at 40 Hz frequency, yielding isotropic lines of about 30–50 Hz linewidth at half-intensity ($\Delta\nu_{1/2}$) after application of a 25 Hz line-broadening. Typical experimental parameters were: 7 μs $\pi/2$ pulses, 6 s recycle time, 100 scans, 5 kHz spectral window and gated broadband proton decoupling. Experiments were carried out in the presence of an external reference containing HPO_4^{2-} (41 mM, 80 μl, pH 10.5). Chemical shift values are given relative to 85% H_3PO_4. Peak area integration was performed using standard Bruker programs. Reference peak area was used to calculate sample mole number and concentration, with 10% accuracy.

3. Results

Micellar systems

^{31}P-NMR spectra of micelles made of a single phospholipid (PE, PS or PC) in the absence (Fig. 1, left) and presence of $HgCl_2$ (Fig. 1, right, $R_i = 2.4$) show well-resolved single NMR lines. The outermost left signal (+3.2 ppm) corresponds to the phosphate external reference (R). Isotropic chemical shift values (δ) for PE, PS and PC are +0.30, +0.15 and –0.40 ppm, respectively, in the absence of mercury (Table 1). It is worth mentioning that signal area and linewidth for each lipid micellar phase were constant over periods of 3 days, indicating that no lipid degradation occurred during that time (data not shown). $HgCl_2$ addition at $R_i = 2.4$ induces an important ^{31}P-NMR peak area decrease, with a stronger effect for PE and PS compared to PC (Fig. 1, right). Formation of a white precipitate is observed with all three phospholipids upon mercury addition. However, they quickly disappear under stirring, except for PE. No changes are observed for PE and PC chemical shifts, whereas a +0.30 ppm upfield shift is detected for PS in the presence of $HgCl_2$ (Table 1). Time-dependence of $HgCl_2$ effects on PE, PS and PC NMR signals was studied (Fig. 2, $R_i = 2.4$). About 85% of the total peak area decrease occurs in the first 15 min after $HgCl_2$ addition, then a slow decrease is observed for 120 min. At longer times, peak areas show a tendency to plateau and are nearly constant over 24 hours (data not shown). A pseudo-first other model, $A(t) = A_0 e^{-t/\beta}$, can be applied to fit the initial fast kinetic phase, with $A_0 = 100\%$ and $1/\beta$ the rate of peak decrease (in min^{-1}). Similar experiments were carried out with $R_i = 1.6$ and 0.8, and the $1/\beta$ values are reported in Table 2. Peak areas measured well after the fast exponential decrease, at t = 40 min (A_{40}), are also reported in Table 2. Note that inorganic mercury has maximal effect on PE, intermediate on PS and minimal on PC both for $1/\beta$ and A_{40} values, whereas the delay before the

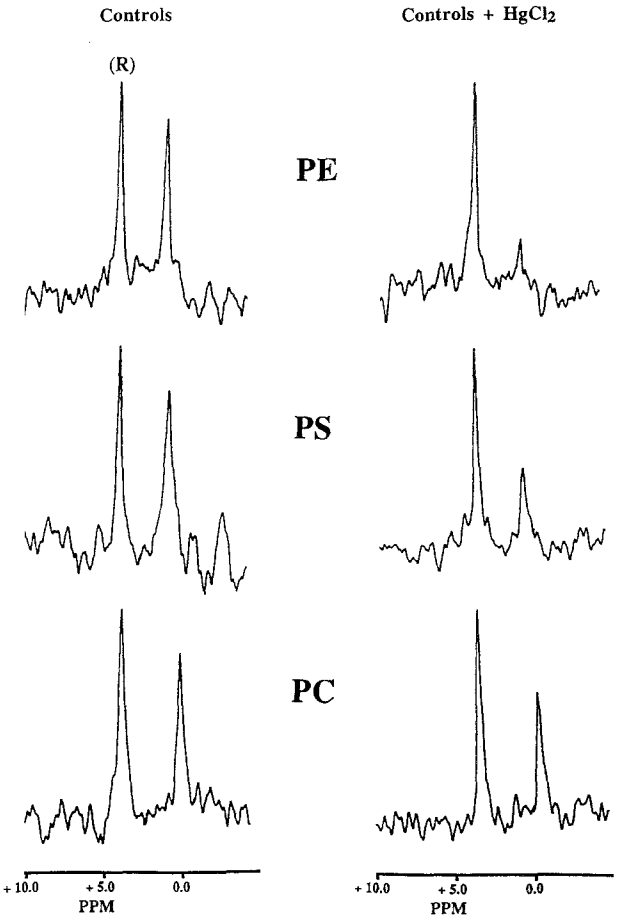

Fig. 1 ^{31}P-NMR high resolution spectra of one-lipid micelles of PE, PS and PC (15 mM), in the absence and presence of $HgCl_2$ ($R_i = 2.4$). Left spectra are controls, while spectra on the right were acquired 40 min after $HgCl_2$ addition. Left NMR signal (*R*) corresponds to the external reference (HPO_4^{2-}, 80 mM, pH 10.5). Chemical shifts are expressed relative to 85% H_3PO_4

Table 1 ^{31}P-NMR isotropic chemical shift values, δ, of phospholipid micelles in the presence and absence of Hg(II)

	PE	PS	PC
Controls	+0.30	+0.15	–0.40
One-lipid micelles + Hg	+0.30	+0.45 ($\Delta\delta$ = +0.30)	–0.40
Two-lipid micelles + Hg	+0.40 ($\Delta\delta$ = +0.10)	+0.45 ($\Delta\delta$ = +0.30)	–0.45

Chemical shift values are measured in ppm, relative to 85% H_3PO_4 (0 ppm). All values are given with a 0.10 ppm accuracy. Significative peak displacements observed upon $HgCl_2$ addition are denoted with $\Delta\delta$. Two-lipid micelles results are similar for both PL1 + PL2 and PL1/PL2 preparations

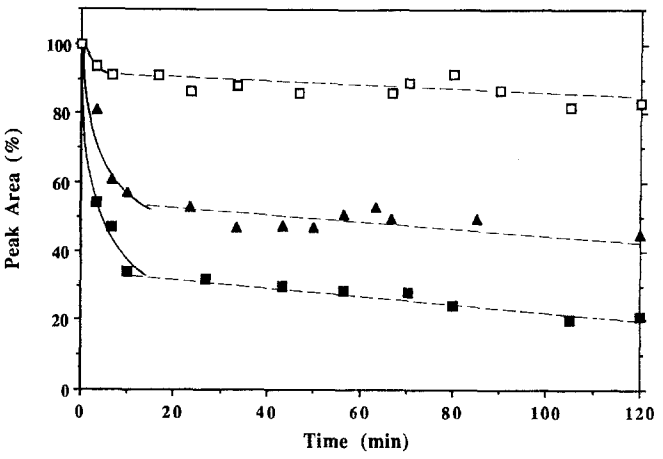

Fig. 2 ^{31}P-NMR peak area decrease (in %) as a function of time, after $HgCl_2$ addition ($R_i = 2.4$), for PE (■); PS (▲); and PC (❑) micelles. *Solid lines* represent the best fits according to pseudo first order kinetics (see text). *Dashed lines* are drawn to help read the figure

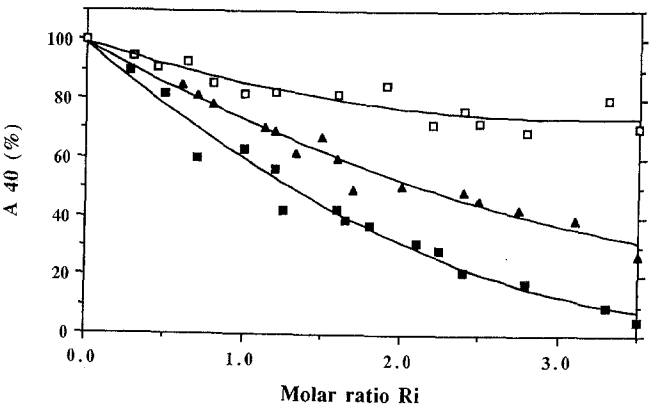

Fig. 3 ^{31}P-NMR peak area at t = 40 min (A_{40}, in %), as a function of R_i, for PE (■); PS (▲); and PC (❑) micelles. Data points are the means of 2 to 5 independent measurements. *Solid lines* are drawn to help read the figure

Table 2 Kinetic parameters for the effect of $HgCl_2$ on phospholipid micelles

	PE		PS		PC	
	A_{40} [a]	$1/\beta$ [b]	A_{40}	$1/\beta$	A_{40}	$1/\beta$
$R_i = 0.8$	77	$1.4\ 10^{-2}$	80	$9.0\ 10^{-3}$	93	$5.8\ 10^{-4}$
$R_i = 1.6$	43	$5.0\ 10^{-2}$	62	$1.6\ 10^{-2}$	87	n.d.
$R_i = 2.4$	28	$1.0\ 10^{-1}$	48	$5.9\ 10^{-2}$	82	$1.4\ 10^{-2}$

[a] A_{40} is the peak area value at t = 40 min (in %), with 10% accuracy
[b] $1/\beta$ is the pseudo-first order rate of peak area decrease (in min^{-1}), with 10% accuracy. (*n.d.*: not determined)

slow kinetic phase (about 15 min) does not depend on the lipid or R_i. Effects of wide R_i variations on PE, PS and PC peak areas measured at t = 40 min are presented in Fig. 3 and reveal qualitatively similar results. Each phospholipid studied shows a non-linear, progressive peak area decrease with increasing R_i. Quantitatively, the decrease in area always occurs in the order PE > PS > PC for a specific R_i. No significant changes in peak linewidth occur for any of the R_i investigated (data not shown). To validate the observed Hg(II)-PC binding, which had not been previously reported in ^{199}Hg-NMR studies (Delnomdedieu et al. 1992), micelles of the synthetic phospholipid DPPC were also tested under identical conditions ($R_i = 2.4$) and a similar 15–20% peak area decrease ($A_{40} = 80$–85%) is observed with micelles of both DPPC and the natural phospholipid egg PC (data not shown).

When two different phospholipids PL1 and PL2 are mixed together, whatever the micelle preparation mode, both PE and PC or PS and PC systems give well-resolved ^{31}P-NMR signals (Fig. 4, left and Table 1). Unfortunately, PE and PS isotropic chemical shifts only differ by 0.15 ppm, a value too close to the average peak linewidth

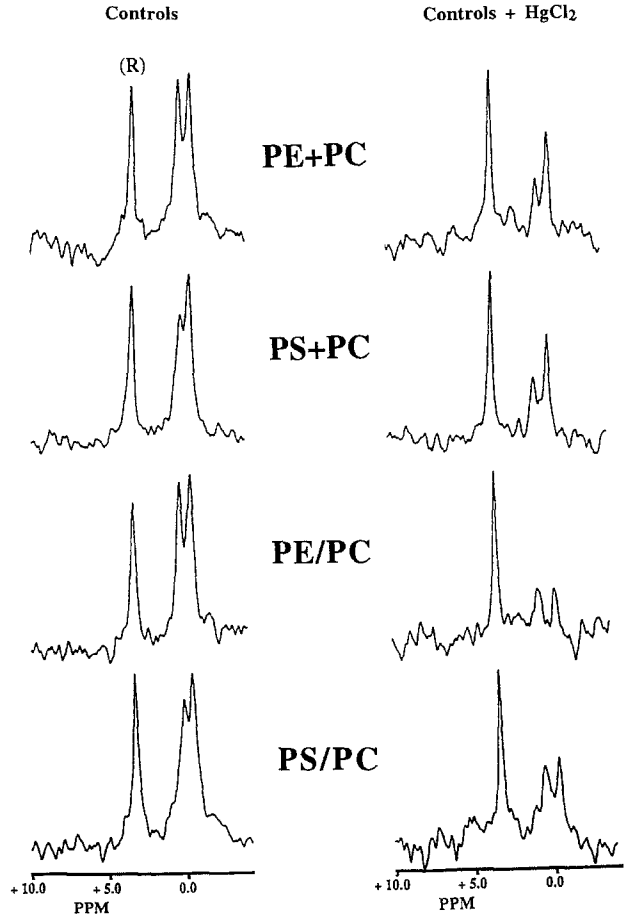

Fig. 4 ^{31}P-NMR high resolution spectra of two-lipid micelles (15 mM each), prepared as mixtures (PL1 + PL2) or as mixed micelles (PL1/PL2), in the absence and presence of $HgCl_2$ ($R_i = 1.6$). Left spectra are controls, and spectra on the right were acquired 40 min after $HgCl_2$ addition. Left NMR signal (*R*) corresponds to the external reference, as in Fig. 1. Chemical shifts are expressed relative to 85% H_3PO_4

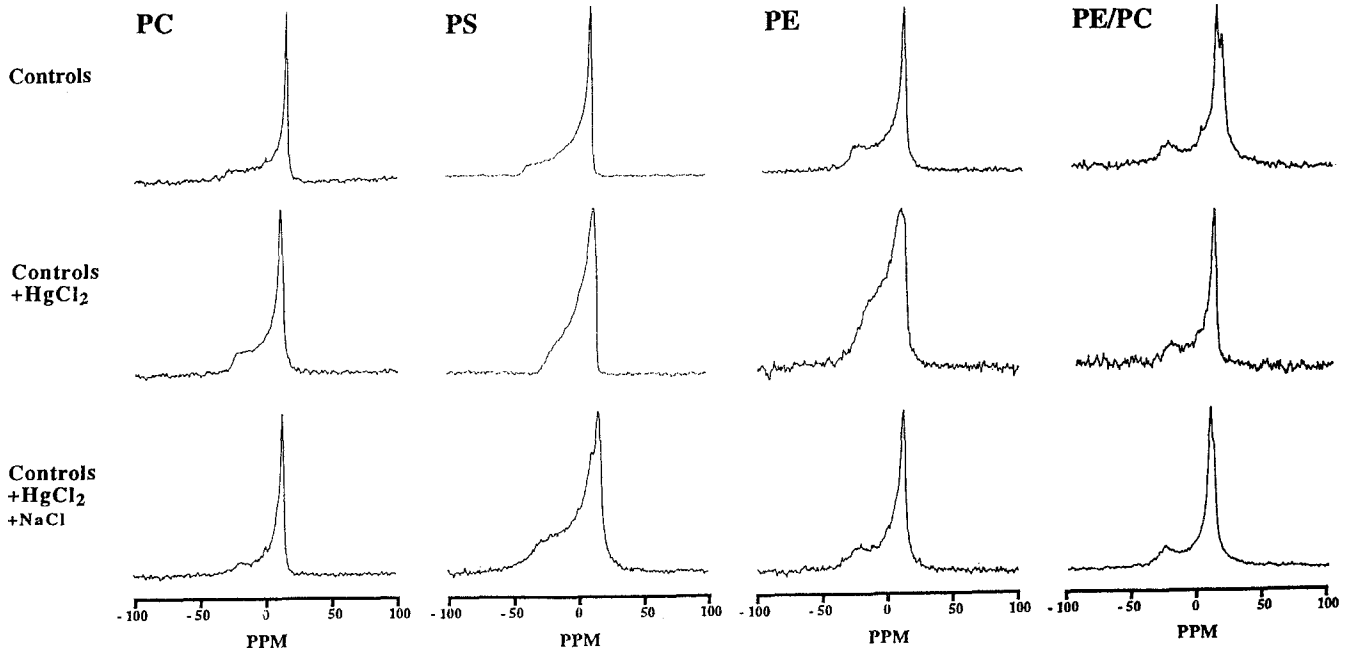

Fig. 5 ^{31}P-NMR powder spectra of phospholipid multilamellar vesicles, in the absence and presence of $HgCl_2$ and NaCl. Top spectra are controls, middle spectra were acquired after $HgCl_2$ addition ($R_i = 2.4$) and equilibration, and bottom spectra were acquired immediately after NaCl (6.2 M) addition to PL + $HgCl_2$ samples

to allow sufficient peak separation and individual integration of the two NMR signals. Samples containing PE and PS were therefore not prepared. When $HgCl_2$ ($R_i = 1.6$) is added to PL1 + PL2 samples immediately after recording controls (15 min), ^{31}P-NMR spectra recorded 40 min later (Fig. 4, top right) yield individual phospholipid signal areas (A_{40}) similar to those observed at the same R_i with single lipid preparations (Fig. 3). At variance, for $HgCl_2$ addition to mixed PE/PC and PS/PC micelles, both lipids show a simultaneous decrease of ^{31}P-NMR signals (Fig. 4, bottom right). This peak area reduction is R_i-dependent, leading to A_{40} values for both (PC and PE) or (PC and PS) signals similar to those obtained at the same R_i with PE or PS single micelles, respectively (Fig. 3). Interestingly, when $HgCl_2$ is added one hour after mixing PE + PC or PS + PC micelles together and NMR spectra taken 40 min later, the system behaves as reported for mixed micelles (PE/PC and PS/PC, respectively). It is also noteworthy that isotropic chemical shifts, in the presence of Hg(II), show variations very similar to those observed with individual PC or PS lipid micelles (Table 1), except for PE where a slight increase of the resonance is observed.

Phospholipid multilamellar vesicles

^{31}P-NMR powder spectra of PC, PS, PE and PE/PC MLV in the absence and presence of $HgCl_2$ ($R_i = 2.4$) are shown in Fig. 5. Spectra taken in the presence of both Hg(II) and NaCl (6.2 M) are also shown in this figure. All spectra for controls (Fig. 5, top) show a well-defined, axially symmetric lineshape characteristic of a fluid L_α phase (Seelig 1978). Chemical shift anisotropy ($\Delta\sigma$) was measured between the low-field shoulder and high-field peak and is reported in Table 3. Two different $\Delta\sigma$ values are observed with PE/PC systems, corresponding to the overlapping spectra of PE ($\Delta\sigma = -40$ ppm) and PC ($\Delta\sigma = -44$ ppm), respectively. Delnomdedieu et al. (1992) have shown that $HgCl_2$-PL dispersions need several hours to equilibrate, so ^{31}P-NMR spectra were recorded as a function of time. The middle row of Fig. 5 shows spectra after mercury addition, at equilibrium, i.e. when lineshape changes are no longer detected by NMR. This is achieved after 4 hours for PC and mixed PE/PC samples and up to 24 hours for PS and PE. A significant decrease of $\Delta\sigma$ values for PC, PS and PE/PC dispersion spectra is observed in the presence of $HgCl_2$, while no marked change is detected for PE. It is noteworthy that Hg(II) addition to the initially resolved PE/PC system leads to a unique $\Delta\sigma$ value (Table 3). A marked increase is observed in the powder pattern linewidth of PS and PE spectra (Fig. 5, middle row) and it must be mentioned that Hg(II)-PL samples sediment down in the

Table 3 ^{31}P-NMR chemical shift anisotropy ($\Delta\sigma$) values of phospholipid multilamellar vesicles in the presence and absence of Hg(II)

	PE	PS	PC	PE/PC (1/1)
Controls	–40	–49	–44	–40/–44
Controls + Hg	–41	–34	–34	–34
Controls + Hg + 6.2 M NaCl	–37	–49	–44	–41/–43

Chemical shift anisotropy values are measured in ppm, at 296 K. All values are given with a 3 ppm accuracy. $HgCl_2$ was added at $R_i = 2.4$. When two overlapping powder spectra are observed, both $\Delta\sigma$ values are reported

NMR tubes after a few hours, forming solid-like precipitates. Addition of NaCl 6.2 M to Hg(II)-PL samples induces an immediate disappearance of the precipitates and a fast (15 min) reversal to the L_α phase, as revealed by ^{31}P-NMR, though spectral lineshapes do not perfectly match controls, especially for PS (Fig. 5: bottom row, compared to top). The observed chemical shift anisotropy values of all lipid dispersions are also restored, within the experimental error, to their initial mercury-free values upon NaCl addition (Table 3).

Figure 6 shows the time evoluation of ^{31}P NMR spectra after addition of $HgCl_2$ ($R_i = 2.4$) to both the lamellar (left column spectra) and the hexagonal type II (right column spectra) phases of PE dispersions. When mercury is added to the lamellar phase (T = 296 K), one notices the growing of an isotropic spectral component after incubation for $t \geq 3$ h. This new component disappears after 24 h leading to a new lamellar-type powder pattern with slightly reduced $\Delta\sigma$ and marked increase in powder pattern linewidth. $HgCl_2$ addition to the hexagonal phase (T = 318 K) also leads to the appearance of an isotropic spectral component, for $t \geq 2$ h which disappears after $t \geq 8$ h to the benefit of a new lamellar-type powder pattern with spectral characteristics similar to those obtained at T = 296 K, for $t \geq 24$ h, after $HgCl_2$ addition. Increase in temperature to T = 333 K does not restore the hexagonal type II phase (not shown). Thin layer chromatography analysis of samples after completion of experiments showed that no significant PE degradation had occurred.

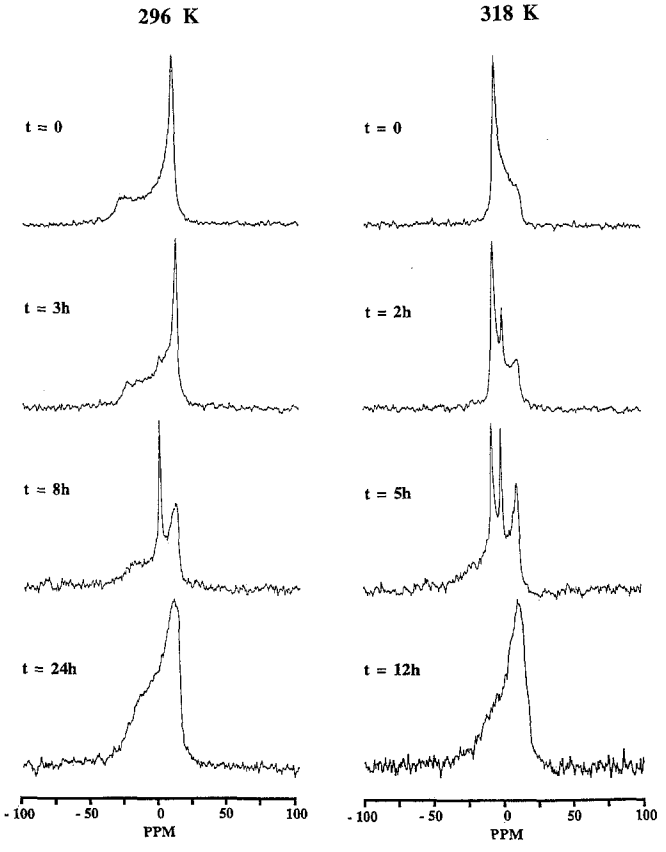

Fig. 6 ^{31}P-NMR powder spectra of PE multilamellar vesicles as a function of time and temperature, in the absence and presence of $HgCl_2$. Top spectra are controls, other spectra were acquired after $HgCl_2$ addition ($R_i = 2.4$). Left spectra were acquired at T = 296 K and right spectra at T = 318 K

4. Discussion

The above results demonstrate that mercury chloride clearly interacts with phospholipid systems independently of the macromolecular state of organization, i.e. micelles or multilamellar dispersions. Interactions with micelles affords the determination of lipid selectivity and provides rates of binding whereas complexation with phospholipid membranes promotes changes in membrane structure and dynamics. All these points will be discussed in the following.

Phospholipid micelles

Prior to discussing the implications of $HgCl_2$ binding to micelles, it is worth commenting from the NMR viewpoint on the decrease in area of the phospholipid isotropic line upon mercury addition. The observation of sharp isotropic NMR lines indicates the presence of small objects such as lipid micelles (radius <50 Å) with rotational correlation times less than a nanosecond. Formation of larger objects such as extended bilayers or very large phospholipid vesicles (radius >5000 Å), with correlation times greater than a millisecond, gives rise to very wide anisotropic lines, i.e. powder-patterns of 5–20 kHz width (Burnell et al. 1980). The ^{31}P-NMR isotropic line observed in our experiments can thus be related to the fraction of phospholipids engaged in small "soluble" micelles (Tacnet et al. 1991) and the isotropic signal decrease observed upon $HgCl_2$ addition is explained by the involvement of some lipids in the formation of a large "insoluble" complex with mercury, in slow exchange (on the NMR time scale) with the free micelle fraction. This phase yields a very broad ^{31}P-NMR powder spectrum that cannot be detected with the acquisition parameters used for micelles. A decrease in the isotropic line area can therefore be related to the amount of phospholipid tightly involved with mercury. This insoluble lipid phase could result from linkage by Hg(II) to several distinct micelles, forming by extension a three-dimensional "network". This hypothesis implies a stoichiometry of two or more phospholipid ligands per Hg(II), which is consistent with previous results (Delnomdedieu et al. 1992). Binding and aggregation of several phospholipids by $HgCl_2$ was also invoked to interpret the mercury-induced rigidification of model and natural membranes (Delnomdedieu et al. 1989; Delnomdedieu and Allis 1993). Note that $HgCl_2$ binding to PE must be especially strong and extensive, since it results in a stable and visible precipitate.

The initial rate for micellar aggregation ($1/\beta$) increases at high R_i (Fig. 3 and Table 2), which is consistent with the pseudo first-order kinetic model. Moreover, head-

group specificity also influences $1/\beta$ values in the order PE > PS > PC, similar to the affinity order observed when comparing A_{40} values. Quantitatively, 85% of $HgCl_2$ binding to the phospholipids takes place during the first 15 min. These kinetics are interestingly very similar to those reported for inorganic mercury adsorption on muscular cells by Rothstein (1976), suggesting that Hg(II) binding to phospholipids could be at least partly responsible for the metal adsorption on whole biological membranes.

Chemical shifts and linewidths of the phospholipid isotropic signals are nearly unchanged upon $HgCl_2$ addition (Table 1), indicating that no direct mercury binding to the lipid phosphate group occurs in the soluble fraction, as such a binding would greatly perturb the phosphate electronic environment, causing large changes of the δ values and relaxation parameters (Dennis and Plückhthun 1984). However, formation of soluble Hg(II)-phospholipid complexes involving other reactive groups, and especially amines of the polar heads, would have a reduced effect on the distant phosphate and, consequently, on the lipid δ values. The small chemical shift changes observed with PS micelles in the presence of $HgCl_2$ reveal the existence of a soluble Hg(II)-PS species. Formation of similar complexes with PE or PC cannot be inferred nor excluded from ^{31}P-NMR measurements: unchanged δ values could result from a greater distance between the phosphate and the mercury binding sites in PE and PC than in PS, due to different conformations of these headgroups in the presence of $HgCl_2$.

Inorganic mercury interactions with phospholipids are highly dependent on the headgroup nature. Reactivity order as observed by ^{31}P-NMR for insoluble phase formation (Fig. 3) can be related to ^{199}Hg-NMR studies of mercury-lipid complex precipitation. A higher formation constant was found for $Hg(PE)_3$ as compared to $Hg(PS)_3$ (Delnomdedieu et al. 1992). However, previous studies failed to detect PC-mercury complexes, possibly because ^{199}Hg-NMR experimental conditions needed high mercury concentrations (0.1 M) which might have masked any small decrease of PC and free Hg concentrations. Similar ^{31}P-NMR results obtained herein with natural egg-yolk PC (lecithin) and synthetic DPPC actually demonstrate a choline-specific $HgCl_2$ binding, independent of lipid chain composition. $HgCl_2$ does, however, display a smaller apparent affinity for PC than for PE and PS primary amine groups, the choline quaternary ammonium ion being the most probable low-affinity mercury binding site on PC.

When two different lipid micellar samples are mixed together, $HgCl_2$ specifically binds to the most reactive lipid (Fig. 4, top), i.e., PC does not efficiently compete with PE or PS. In addition, its presence does not significantly affect the reaction kinetics and thermodynamic parameters observed for single lipid micelles. Unfortunately, PE/PS competition could not be observed, as already mentioned, owing to peak overlapping of the phospholipid ^{31}P-NMR signals. When micelles composed of one strongly reactive and one weakly reactive phospholipid are tested for $HgCl_2$ effects (Fig. 4, bottom), both lipid ^{31}P-NMR signals strongly decrease. This co-precipitation was expected according to the network model of immobilized micelles, whereby motional decrease of PC molecules incorporated in mixed micelles should be induced by $HgCl_2$ reaction with either PE or PS. It also demonstrates that, in the micellar phase, complete lipid aggregation is efficiently induced by $HgCl_2$ binding to a specific micelle component, i.e., no phase separation happens that would result from the extraction of PE or PS and leave PC in the soluble fraction. Also remarkable is the time-dependent evolution of mixtures of one-lipid micelles towards the behavior of heterogenous mixed micelles, demonstrating that fast phospholipid exchange occurs between individual micelles at room temperature. After one hour, phospholipid redistribution abolishes any apparent specificity of mercury for PE or PS versus PC in mixture of one-lipid micelles.

Phospholipid membranes

The ^{31}P-NMR $\Delta\sigma$ value decrease observed upon $HgCl_2$ addition ($R_i = 2.4$) to PS, PC and mixed PE/PC MLV (Fig. 5: middle and Table 5) reveals either an increase of phosphate local motions or a change in the headgroup tilt angle relative to the bilayer normal (Seelig 1978; Rajan et al. 1981; Dufourc et al. 1992). It is possible that Hg(II) complexation disrupts inter-headgroup interactions (electrostatic pairing or hydrogen bonding) that otherwise restrict the axial and lateral motions of the phospholipid molecule: similar results have been reported for lanthanide interactions with DMPS liposomes (Petersheim and Sun 1989). Surface covalent binding of Hg(II) could also force a reorientation of the phospholipid headgroups. Note that these two mechanisms are not mutually exclusive, though micelle results demonstrating tight Hg(II)-PL interactions favor the reorientation hypothesis. In addition, the overall increase in powder pattern linewidth of PS dispersions in the presence of $HgCl_2$ reflects a decrease of the slow lipid motions (Dufourc et al. 1992). Resulting ^{31}P-NMR spectra are then typical of a gel-lamellar phase, except for their reduced $\Delta\sigma$ value. Lipid collective motions and lateral diffusion, and therefore membrane fluidity, thus appear to be restricted upon mercury-induced surface bridging of lipid headgroups, by the same mechanisms that cause micelle immobilization, i.e. intermolecular network formation.

In the presence of $HgCl_2$, spectra of both PE lamellar fluid and hexagonal phases slowly disappear and are replaced by a spectrum typical of a lamellar gel phase. As with PS, the very broad powder pattern linewidth is indicative of a mostly "frozen" membrane of greatly reduced fluidity. Moreover, the observed transient isotropic line reveals the formation of small-sized objects, micelles or small unilamellar vesicles (SUV), implying different molecular mechanisms for $HgCl_2$ interactions with PE and PS and a specific Hg(II) position in PE bilayers, compared to the other phospholipid dispersions. Isotropic line formation has been reported for calcium binding to negatively charged cardiolipin dispersions and was interpreted as metal-induced membrane fusion (Schanck and Deleers 1993). In the same way, one may think that $HgCl_2$ is able to destructure PE lamellar fluid and hexagonal phases, in-

ducing a transitory isotropic phase that is highly temperature-sensitive, but ultimately forcing the membrane into a rigid, gel-like lamellar phase that completely prevents the temperature-induced L_α-to-H_{II} transition (Fig. 6). This is especially interesting from a toxicological point of view, since the hexagonal phase is supposed to be a necessary intermediate step during membrane fusion, exo- and endocytoses, and for lipid turnover (Cullis and de Kruijff 1978). $HgCl_2$ binding to biomembranes would certainly affect these essential cell functions. Also, it is tempting to relate the gel-like phases observed with PS and PE bilayers to the fluidity loss induced by mercurials upon many biomembranes. Membrane rigidification greatly reduces its exchange properties and perturbs the activity of membrane proteins as well. However, it is noteworthy that PE dilution in a less-reactive PC bilayer offers protection from the most drastic of mercury effects: no gel-like or isotropic phase formation is observed upon $HgCl_2$ addition to PE/PC MLV (Fig. 5), indicating that no phase separation occurs between PE and PC. This result does not necessarily preclude PE binding, network formation, and the consecutive blocking of H_{II} phase formation. Thermotropic stability of the Hg(II)-PE spectra supports the model of a gel-like structure that hinders all membrane phase transitions. Fluorescence polarization studies of PE and PS dispersions revealed a loss of the main L_β to L_α phase transition upon inorganic mercury binding at $R_i = 2.5$ (Delnomdedieu et al. 1989). However, ^{31}P-NMR results demonstrate that Hg(II) complexation does not cause a loss of the bilayer structure for PS, even though Hg(II)-PS and Hg(II)-PE gel-like phases display similar thermotropic behaviors. The NaCl-induced reversal of Hg(II)-PL systems to a "mercury-free" L_α phase (Fig. 5: bottom) corroborates previous ^{199}Hg-NMR data that showed a complete removal of bound Hg(II) upon chloride addition (Delnomdedieu et al. 1992). This phenomenon has already been accounted for by the formation of the thermodynamically stable $HgCl_4^{2-}$ species which does not react with lipids. This reinforces the idea that chemical speciation, i.e. the formation of Hg complexes depending upon physicochemical conditions of the medium, is a key factor for mechanisms that are conditioning mercury toxicity in the environment.

^{31}P-NMR results suggest that metal ion binding to a specific, high-affinity lipidic membrane component (PE and PS in the case of inorganic mercury) could cause extensive, unspecific lipid aggregation, inducing large disturbances such as loss of membrane integrity or fluidity, and dysfunction of associated proteins. PE and PS indeed represent 45% of the total phospholipids in human red blood cells and are located mainly at the membrane inner side (Rothstein 1981). Inner lipidic sites are accessible to easily diffusing, uncharged species such as $HgCl_2$, and by complexation with mercury they could promote severe membrane and cell damage, in addition to the well-known (and very important) mercury effects on proteic thiols and disulfide bridges (Gutknecht 1981; Rothstein 1981). Because of the high complexity and diversity of the biotic factors, it is not always possible to relate the macroscopic toxicological effects of metals observed at the cell and organism levels to specific molecular interactions and chemical speciation mechanisms. Nonetheless, fluorescence polarizaton studies of inorganic mercury binding to rat erythrocyte ghosts have demonstrated a Hg(II)-induced decrease of membrane fluidity, the effect being very dependent on mercury chemical speciation (Delnomdedieu and Allis 1993). Recent toxicological studies confirmed that Hg(II) is mainly localized in vivo at the membrane level. By interacting strongly with thiols and aminophospholipids, Hg(II) thus appear to promote immediate damage to the cell, while organic species such as $CH_3Hg(II)$ that also easily cross biomembranes would transfer to and accumulate in the organism, for later toxicological effects, for instance on the central nervous system (Clarkson 1994).

References

Bevan Dr, Worrel WJ, Barfield KD (1983) The interaction of Ca^{2+}, Mg^{2+}, Zn^{2+}, Cd^{2+}, and Hg^{2+} with phospholipid bilayer vesicles. Colloids Surf 6:365–376

Boadi WY, Urbach J, Brandes JM, Yannai S (1992) In vitro exposure to mercury and cadmium alters term human placental membrane fluidity. Toxicol Appl Pharmacol 116:17–23

Burnell EE, Cullis PR, de Kruijff B (1980) Effects of tumbling and lateral diffusion on phosphatidylcholine model membrane ^{31}P-NMR lineshapes. Biochim Biophys Acta 603:63–69

Chávez E, Holguín JA (1988) Mitochondrial calcium release as induced by Hg^{2+}. J Biol Chem 263:3582–3587

Clarkson TW (1994) The toxicology of mercury and its compounds. In: Watras CJ and Huckabee JW (eds) Mercury pollution, integration and synthesis. Lewis Publishers, Boca Raton, pp 631–641

Cullis PR, de Kruijff B (1978) The polymorphic phase behaviour of phosphatidylethanolamines of natural and synthetic origin. Biochim Biophys Acta 513:31–42

Delnomdedieu M, Boudou A, Desmazès JP, Georgescauld D (1989) Interaction of mercury chloride with the primary amine group of model membranes containing phosphatidylserine and phosphatidylethanolamine. Biochim Biophys Acta 986:191–199

Delnomdedieu M, Boudou A, Georgescauld D, Dufourc EJ (1992) Specific interactions of mercury chloride with membranes and other ligands as revealed by mercury-NMR. Chem-Biol Interact 81:243–269

Delnomdedieu M, Allis JW (1993) Interaction of inorganic mercury salts with model and red cell membranes: importance of lipid binding sites. Chem-Biol Interact 88:71–87

Dennis EA, Plückhthun A (1984) Phosphorus-31 NMR of phospholipids in micelles. In: Gorenstein DG (ed) Phosphorus-31 NMR: principles and applications. Academic Press, London, pp 423–446

Dufourc EJ, Mayer C, Stohrer J, Althoff G, Kothe G (1992) Dynamics of phosphate head group in biomembranes. Biophys J 61: 42–57

Farrell RE, Germida JJ, Ming Huang PM (1993) Effects of chemical speciation in growth media on the toxicity of mercury(II). Appl Environm Microbiol 59:1507–1514

Foulkes EC, Bergman D (1993) Inorganic mercury absorption in mature and immature rat jejunum: transcellular and intercellular pathways in vivo and in everted sacs. Toxicol Appl Pharmacol 120:89–95

Gutknecht J (1981) Inorganic mercury (Hg^{2+}) transport through lipid bilayer membranes. J Membr Biol 61:61–66

Kinter WB, Pritchard JB (1977) Altered permeability of cell membranes. In: Handbook of Physiology (section 9): Reactions to environmental agents. Williams and Wilkins, London, pp 563–573

Petersheim M, Sun J (1989) On the coordination of La^{3+} by phosphatidylserine. Biophys J 55:631–636

Rajan S, Kang SY, Gutowsky HS, Oldfield E (1981) Phosphorus nuclear magnetic resonance study of membrane structure. J Biol Chem 256:1160–1166

Ralston GB, Crisp EA (1981) The action of organic mercurials on the erythrocyte membrane. Biochim Biophys Acta 649:98–104

Rance M, Byrd RA (1983) Obtaining high-fidelity spin-1/2 powder spectra in anisotropic media: phase-cycled Hahn echo spectroscopy. J Magn Res 52:221–240

Ribarov SR, Benov LC (1981) Relationship between the hemolytic action of heavy metals and lipid peroxidation. Biochim Biophys Acta 640:721–726

Rothstein A (1976) Cell membrane as site of action of heavy metals. In: Brönner F, Kleinzeller A (ed) Current topics in membrane transport. Academic Press, New York, pp 1–76

Rothstein A (1981) Mercurials and red cell membranes. In: The function of red blood cells: erythrocyte pathobiology. Alan R Liss, New York, pp 105–131

Schanck A, Deleers M (1993) ^{31}P-NMR study of the parameters influencing the formation of non-bilayer phases in model membrane. Biochem Biophys Res Commun 195:654–658

Schecher WD, McAvoy DC (1991) Mineql. 2.23 program. Environmental Research Software, Cincinnati

Seelig J (1978) ^{31}P nuclear magnetic resonance and the head group structure of phospholipids in membranes. Biochim Biophys Acta 515:105–140

Sharma DC, Davis PS, Sharma PK (1981) Studies in search of modifiers of the toxicity of mercurials and speculations on its biochemical mechanism. Biochem Pharmacol 30:3105–3107

Shinada M, Muto H, Takizawa Y (1991) In vitro interaction of selected phospholipid species with mercuric chloride using Fourier transform ^{1}H-NMR, Bull Environm Contam Toxicol 47:350–354

Singleton WS, Gray MS, Brown ML, White JL (1965) Chromatographically homogenous lecithin from egg phospholipids. J Am Oil Chem Soc 42:53–56

Stáry J, Kratzer K (1989) Mechanism of the cumulation of mercury species in alga *Hydrodictyon reticulatum*. Toxicol Environm Chem 22:197–202

Tacnet F, Ripoche P, Roux M, Neumann JM (1991) ^{31}P-NMR study of pig intestinal brush-border membrane structure: effect of zinc and cadmium ions. Eur Biophys J 19:317–322